EFFECT OF THE BOUNDARY CONDITIONS ON THE VIBRATIONS OF FUNCTIONALLY GRADED SHELLS

Angelo Oreste Andrisano
Department of Mechanical and Civil Engineering,
University of Modena and Reggio Emilia, Italy
E-mail: angelooreste.andrisano@unimore.it

Francesco Pellicano
Department of Mechanical and Civil Engineering,
University of Modena and Reggio Emilia, Italy
E-mail: francesco.pellicano@unimore.it

Matteo Strozzi
Department of Mechanical and Civil Engineering,
University of Modena and Reggio Emilia, Italy
E-mail: matteo.strozzi@unimore.it

Abstract. *In this paper, the effect of the boundary conditions on the nonlinear vibrations of functionally graded (FGM) cylindrical shells is analyzed. The Sanders-Koiter theory is applied to model the nonlinear dynamics of the system in the case of finite amplitude of vibration. The shell deformation is described in terms of longitudinal, circumferential and radial displacement fields. Simply supported, clamped and free boundary conditions are considered. The displacement fields are expanded by means of a double mixed series based on Chebyshev polynomials for the longitudinal variable and harmonic functions for the circumferential variable. Numerical analyses are carried out in order to characterize the nonlinear response when the cylindrical shell is subjected to a harmonic external load; a convergence analysis is carried out by considering a different number of axisymmetric and asymmetric modes. The analysis is focused on determining the nonlinear character of the response as the boundary conditions of the shell vary.*

Keywords*: functionally graded, cylindrical shells, nonlinear vibrations*

1. INTRODUCTION

Functionally graded materials (FGMs) are composite materials obtained by combining and mixing two or more different constituent materials, which are distributed along the thickness in accordance with a volume fraction law. Most of the FGMs are employed in the high-temperature environments because of their heat shielding capacity.

The idea of FGMs was first introduced in 1984/87 by a group of Japanese material scientists [1]. They studied many different physical aspects such as temperature and thermal stress distributions, static and dynamic responses.

Loy et al. [2] analyzed the vibrations of the circular cylindrical shells made of FGM, considering simply supported boundary conditions. They found that the natural frequencies are affected by the constituent volume fractions and configurations of the materials.

Pradhan et al. [3] studied the vibration characteristics of FGM cylindrical shells made of stainless steel and zirconia, under different boundary conditions. They found that the natural frequencies depend on the material distributions and boundary conditions.

Leissa [4] analyzed the linear dynamics of shells having different topologies, materials and boundary conditions, considering the most important shell theories, such as Donnell, Flugge and Sanders-Koiter.

Yamaki [5] studied buckling and post-buckling of the shells in the linear and nonlinear field, reporting the solution methods, numerical and experimental results.

A modern treatise on the shells dynamics and stability can be found in Ref. [6], where also FGMs are considered.

Pellicano et al. [7] considered the nonlinear vibrations of homogeneous isotropic shells, leading to similar conclusions of the present work.

The method of solution used in the present work was presented in Ref. [8].

In Refs. [9-10] the effect of the boundary conditions on the vibrations of circular cylindrical shells is considered.

In this paper, the effect of the boundary conditions on the nonlinear vibrations of FGM cylindrical shells is analyzed.

The Sanders-Koiter theory is applied to model the nonlinear dynamics of the system in the case of finite amplitude of vibration.

The shell deformation is described in terms of longitudinal, circumferential and radial displacement fields.

The theory considers geometric nonlinearities due to large amplitude of vibration.

Simply supported, clamped and free boundary conditions are considered.

The FGM is made of a uniform distribution of stainless steel and nickel, and the material properties are graded in the thickness direction, according to a volume fraction power-law distribution.

The solution method consists of two steps:

1) linear analysis and eigenfunctions evaluation;

2) nonlinear analysis, using an eigenfunction based expansion.

In the linear analysis, the displacement fields are expanded by means of a double series based on harmonic functions for the circumferential variable and Chebyshev polynomials for the longitudinal variable.

A Ritz based method allows to obtain the approximate natural frequencies and mode shapes (eigenvalues and eigenvectors).

In the nonlinear analysis, the three displacement fields are re-expanded by using the approximate eigenfunctions.

An energy approach based on the Lagrange equations is then considered, in order to reduce the nonlinear partial differential equations to a set of nonlinear ordinary differential equations.

Numerical analyses are carried out in order to characterize the nonlinear response when the shell is subjected to a harmonic external load.

A convergence analysis is carried out on a simply supported cylindrical shell to obtain the correct number of axisymmetric and asymmetric modes able to describe the actual nonlinear behaviour of the shell. Comparisons of nonlinear amplitude-frequency curves of the cylindrical shell with different nonlinear expansions are carried out.

The influence of the boundary conditions on the natural frequencies of the shell is analyzed. A comparison of nonlinear amplitude-frequency curves of the cylindrical shell under various boundary conditions is carried out.

2. EQUATIONS OF FUNCTIONALLY GRADED MATERIALS

A generic material property P_{fgm} of an FGM depends on the material properties and the volume fractions of the constituent materials, and it is expressed in the form [2]

$$P_{fgm}(T,z) = \sum_{i=1}^{k} \widetilde{P}_i(T) V_{fi}(z) \tag{1}$$

where $\widetilde{P}_i$ and V_{fi} are the material property and volume fraction of the constituent material i, respectively.

The material property $\widetilde{P}_i$ of a constituent material can be described as a function of the environmental temperature T(K) by Touloukian's relation [2] (the index i is dropped for the sake of simplicity)

$$\tilde{P}(T) = P_0(P_{-1}T^{-1} + 1 + P_1T + P_2T^2 + P_3T^3) \tag{2}$$

where P_0, P_{-1}, P_1, P_2 and P_3 are the coefficients of temperature of the constituent material.

In the case of an FGM thin cylindrical shell with a uniform thickness h and a reference surface at its middle surface, the volume fraction V_f of a constituent material can be written as [2]

$$V_f(z) = \left(\frac{z + h/2}{h}\right)^p \tag{3}$$

where the power-law exponent p is a positive real number, $(0 \le p \le \infty)$, and z describes the radial distance measured from the middle surface of the shell, $(-h/2 \le z \le h/2)$, see Fig. 1.

For an FGM thin cylindrical shell made of two different constituent materials 1 and 2, the volume fractions V_{f1} and V_{f2} can be written in the following form [3]

$$V_{f1}(z) = 1 - \left(\frac{z + h/2}{h}\right)^p \qquad V_{f2}(z) = \left(\frac{z + h/2}{h}\right)^p \qquad V_{f1}(z) + V_{f2}(z) = 1 \tag{4}$$

where the sum of the volume fractions of the constituent materials is equal to unity.

Young's modulus E, Poisson's ratio ν and mass density ρ are expressed as [3]

$$E_{fgm}(T,z) = \big(E_2(T) - E_1(T)\big)\left(\frac{z + h/2}{h}\right)^p + E_1(T) \tag{5}$$

$$\nu_{fgm}(T,z) = \big(\nu_2(T) - \nu_1(T)\big)\left(\frac{z + h/2}{h}\right)^p + \nu_1(T) \tag{6}$$

$$\rho_{fgm}(T,z) = \big(\rho_2(T) - \rho_1(T)\big)\left(\frac{z + h/2}{h}\right)^p + \rho_1(T) \tag{7}$$

3. SANDERS-KOITER THEORY OF CIRCULAR CYLINDRICAL SHELLS

In Figure 1, an FGM circular cylindrical shell having radius R, length L and thickness h is represented; a cylindrical coordinate system $(O; x, \theta, z)$ is considered in order to take advantage from the axial symmetry of the structure, the origin O of the reference system is located at the centre of one end of the shell. Three displacement fields are represented in Fig. 1: longitudinal $u(x, \theta, t)$, circumferential $v(x, \theta, t)$ and radial $w(x, \theta, t)$.

Elastic Strain Energy, Kinetic Energy, Virtual Work, Damping Forces

The Sanders-Koiter nonlinear theory of circular cylindrical shells, which is an eight-order shell theory, is based on the Love's "first approximation" [4]. The strain components $(\varepsilon_x, \varepsilon_\theta, \gamma_{x\theta})$ at an arbitrary point of the shell are related to the middle surface strains $(\varepsilon_{x,0}, \varepsilon_{\theta,0}, \gamma_{x\theta,0})$ and to the changes in the curvature and torsion $(k_x, k_\theta, k_{x\theta})$ of the middle surface of the shell by the following relationships [5]

$$\varepsilon_x = \varepsilon_{x,0} + zk_x \qquad \varepsilon_\theta = \varepsilon_{\theta,0} + zk_\theta \qquad \gamma_{x\theta} = \gamma_{x\theta,0} + zk_{x\theta} \tag{8}$$

where z is the distance of the arbitrary point of the cylindrical shell from the middle surface and (x, θ) are the longitudinal and angular coordinates of the shell, see Fig. 1.

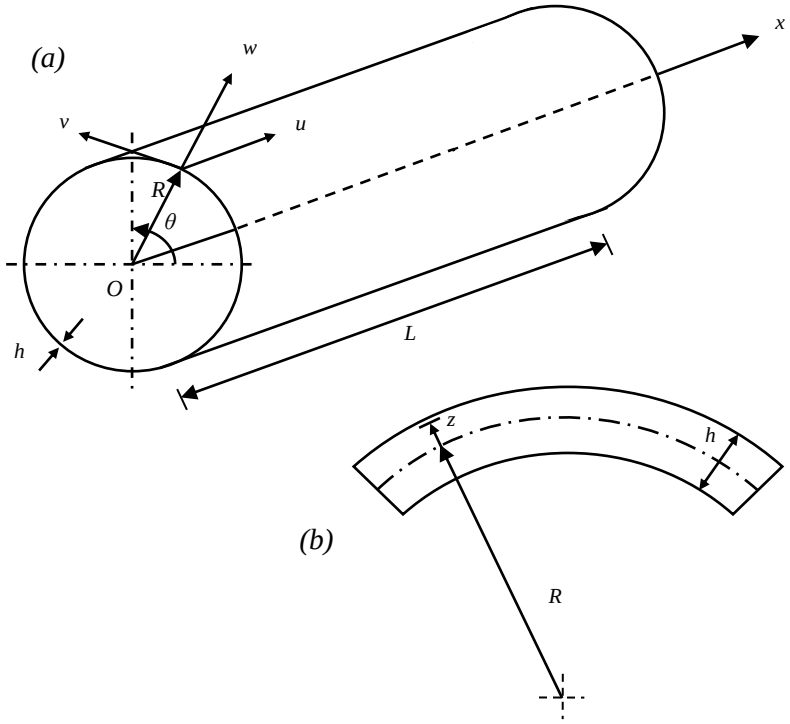

Figure 1. Geometry of the functionally graded cylindrical shell.
(a) Complete shell; (b) cross-section of the shell surface.

The middle surface strains and changes in curvature and torsion are given by [5]

$$\varepsilon_{x,0} = \frac{\partial u}{L\partial\eta} + \frac{1}{2}\left(\frac{\partial w}{L\partial\eta}\right)^2 + \frac{1}{8}\left(\frac{\partial v}{L\partial\eta} - \frac{\partial u}{R\partial\theta}\right)^2 + \frac{\partial w}{L\partial\eta}\frac{\partial w_0}{L\partial\eta}$$

$$\varepsilon_{\theta,0} = \frac{\partial v}{R\partial\theta} + \frac{w}{R} + \frac{1}{2}\left(\frac{\partial w}{R\partial\theta} - \frac{v}{R}\right)^2 + \frac{1}{8}\left(\frac{\partial u}{R\partial\theta} - \frac{\partial v}{L\partial\eta}\right)^2 + \frac{\partial w_0}{R\partial\theta}\left(\frac{\partial w}{R\partial\theta} - \frac{v}{R}\right)$$

$$\gamma_{x\theta,0} = \frac{\partial u}{R\partial\theta} + \frac{\partial v}{L\partial\eta} + \frac{\partial w}{L\partial\eta}\left(\frac{\partial w}{R\partial\theta} - \frac{v}{R}\right) + \frac{\partial w_0}{L\partial\eta}\left(\frac{\partial w}{R\partial\theta} - \frac{v}{R}\right) + \frac{\partial w}{L\partial\eta}\frac{\partial w_0}{R\partial\theta}$$

$$k_x = -\frac{\partial^2 w}{L^2\partial\eta^2} \quad k_\theta = \frac{\partial v}{R^2\partial\theta} - \frac{\partial^2 w}{R^2\partial\theta^2} \quad k_{x\theta} = -2\frac{\partial^2 w}{LR\partial\eta\partial\theta} + \frac{1}{2R}\left(3\frac{\partial v}{L\partial\eta} - \frac{\partial u}{R\partial\theta}\right) \quad (9)$$

where $(\eta = x/L)$ is the nondimensional longitudinal coordinate.

In the case of FGMs, the stresses are related to the strains as follows [6]

$$\sigma_x = \frac{E(z)}{1-\nu^2(z)}(\varepsilon_x + \nu(z)\varepsilon_\theta) \;\; \sigma_\theta = \frac{E(z)}{1-\nu^2(z)}(\varepsilon_\theta + \nu(z)\varepsilon_x) \;\; \tau_{x\theta} = \frac{E(z)}{2\left(1+\nu(z)\right)}\gamma_{x\theta} \quad (10)$$

where $E(z)$ is the Young's modulus and $\nu(z)$ is the Poisson's ratio ($\sigma_z = 0$, plane stress).

The elastic strain energy U_s of a cylindrical shell is given by [6]

$$U_s = \frac{1}{2}LR\int_0^1\int_0^{2\pi}\int_{-h/2}^{h/2}(\sigma_x\varepsilon_x + \sigma_\theta\varepsilon_\theta + \tau_{x\theta}\gamma_{x\theta})\,d\eta d\theta dz \quad (11)$$

The kinetic energy T_s of a cylindrical shell (rotary inertia effect is neglected) is given by [6]

$$T_s = \frac{1}{2}LR\int_0^1\int_0^{2\pi}\int_{-h/2}^{h/2}\rho(z)\,(\dot{u}^2 + \dot{v}^2 + \dot{w}^2)\,d\eta d\theta dz \quad (12)$$

where $\rho(z)$ is the mass density of the shell.

The virtual work W done by the external forces is written as [6]

$$W = LR\int_0^1\int_0^{2\pi}(q_x u + q_\theta v + q_z w)d\eta d\theta \quad (13)$$

with (q_x, q_θ, q_z) as distributed forces in longitudinal, circumferential and radial direction.

The nonconservative damping forces are assumed to be of viscous type and are taken into account by using Rayleigh's dissipation function (viscous damping coefficient c) [6]

$$F = \frac{1}{2}cLR\int_0^{2\pi}\int_0^1(\dot{u}^2 + \dot{v}^2 + \dot{w}^2)\,d\eta d\theta \quad (14)$$

4. VIBRATION ANALYSIS

In order to carry out the dynamic analysis of the shell a two-steps procedure is considered [8]: *i*) the Rayleigh-Ritz method is applied to the linearized formulation of the problem, in order to obtain an approximation of the eigenfunctions; *ii*) the displacement fields are re-expanded using the approximate eigenfunctions, the Lagrange equations are considered in conjunction with the fully nonlinear expression of the potential energy, in order to obtain a set of nonlinear ordinary differential equations in modal coordinates.

Linear Vibration Analysis: Discretization Approach

In order to carry out a linear vibration analysis only the quadratic terms are retained in Eqn. (11). A modal vibration, i.e. a synchronous motion, is obtained in the form [8]

$$u(\eta,\theta,t) = U(\eta,\theta)f(t) \qquad v(\eta,\theta,t) = V(\eta,\theta)f(t) \qquad w(\eta,\theta,t) = W(\eta,\theta)f(t) \tag{15}$$

where $u(\eta,\theta,t), v(\eta,\theta,t), w(\eta,\theta,t)$ are the displacement fields, $U(\eta,\theta)$, $V(\eta,\theta), W(\eta,\theta)$ represent the modal shape, $f(t)$ describes the time law, which is supposed to be the same for each displacement field (synchronous motion hypothesis).

The components of the modal shape are expanded by means of a double mixed series: the periodicity of deformation in the circumferential direction suggests the use of harmonic functions ($\cos n\theta$, $\sin n\theta$), while Chebyshev orthogonal polynomials are considered in the longitudinal direction $T_m^*(\eta)$ [8]

$$U(\eta,\theta) = \sum_{m=0}^{M_u}\sum_{n=0}^{N} \widetilde{U}_{m,n} T_m^*(\eta)\cos n\theta \qquad V(\eta,\theta) = \sum_{m=0}^{M_v}\sum_{n=0}^{N} \widetilde{V}_{m,n} T_m^*(\eta) sin\, n\theta$$

$$W(\eta,\theta) = \sum_{m=0}^{M_w}\sum_{n=0}^{N} \widetilde{W}_{m,n} T_m^*(\eta)\cos n\theta \tag{16}$$

where $T_m^*(\eta) = T_m(2\eta - 1)$, m is the number of longitudinal half-waves, n is the number of nodal diameters and $\left(\widetilde{U}_{m,n}, \widetilde{V}_{m,n}, \widetilde{W}_{m,n}\right)$ are the generalized coordinates.

Simply Supported – Simply Supported Boundary Conditions

Simply supported – simply supported (S – S) boundary conditions are given by [4]

$$w = 0 \qquad v = 0 \qquad M_x = 0 \qquad N_x = 0 \qquad \text{for} \quad \eta = 0,1 \tag{17}$$

The previous conditions imply the following equations [8]

$$\sum_{m=0}^{M_w} \widetilde{W}_{m,n}\, T_m^*(\eta) = 0 \qquad \theta\epsilon[0,2\pi] \qquad n\epsilon[0,N] \qquad \text{for} \quad \eta = 0,1 \tag{18}$$

$$\sum_{m=0}^{M_v} \tilde{V}_{m,n}\, T_m^*(\eta) = 0 \qquad \theta\epsilon[0,2\pi] \qquad n\epsilon[0,N] \qquad \text{for} \quad \eta = 0,1 \qquad (19)$$

$$\sum_{m=0}^{M_w} \widetilde{W}_{m,n}\, T_{m,\eta\eta}^*(\eta) = 0 \qquad \theta\epsilon[0,2\pi] \qquad n\epsilon[0,N] \qquad \text{for} \quad \eta = 0,1 \qquad (20)$$

$$\sum_{m=0}^{M_u} \widetilde{U}_{m,n}\, T_{m,\eta}^*(\eta) = 0 \qquad \theta\epsilon[0,2\pi] \qquad n\epsilon[0,N] \qquad \text{for} \quad \eta = 0,1 \qquad (21)$$

The linear algebraic system given by Eqns. (17) can be solved analytically in terms of the coefficients $\left(\widetilde{U}_{1,n}, \widetilde{U}_{2,n}, \tilde{V}_{0,n}, \tilde{V}_{1,n}, \widetilde{W}_{0,n}, \widetilde{W}_{1,n}, \widetilde{W}_{2,n}, \widetilde{W}_{3,n}\right)$, for $n\epsilon[0,N]$.

Clamped – Clamped Boundary Conditions

Clamped – clamped boundary conditions are given by [4]

$$u = 0 \qquad v = 0 \qquad w = 0 \qquad w_{,\eta} = 0 \qquad \text{for} \quad \eta = 0,1 \qquad (22)$$

The previous conditions imply the following equations [8]

$$\sum_{m=0}^{M_u} \widetilde{U}_{m,n}\, T_m^*(\eta) = 0 \qquad \theta\epsilon[0,2\pi] \qquad n\epsilon[0,N] \qquad \text{for} \quad \eta = 0,1 \qquad (23)$$

$$\sum_{m=0}^{M_v} \tilde{V}_{m,n}\, T_m^*(\eta) = 0 \qquad \theta\epsilon[0,2\pi] \qquad n\epsilon[0,N] \qquad \text{for} \quad \eta = 0,1 \qquad (24)$$

$$\sum_{m=0}^{M_w} \widetilde{W}_{m,n}\, T_m^*(\eta) = 0 \qquad \theta\epsilon[0,2\pi] \qquad n\epsilon[0,N] \qquad \text{for} \quad \eta = 0,1 \qquad (25)$$

$$\sum_{m=0}^{M_w} \widetilde{W}_{m,n}\, T_{m,\eta}^*(\eta) = 0 \qquad \theta\epsilon[0,2\pi] \qquad n\epsilon[0,N] \qquad \text{for} \quad \eta = 0,1 \qquad (26)$$

The linear algebraic system given by Eqns. (22) can be solved analytically in terms of the coefficients $\left(\widetilde{U}_{0,n}, \widetilde{U}_{1,n}, \tilde{V}_{0,n}, \tilde{V}_{1,n}, \widetilde{W}_{0,n}, \widetilde{W}_{1,n}, \widetilde{W}_{2,n}, \widetilde{W}_{3,n}\right)$, for $n\epsilon[0,N]$.

Free – Free Boundary Conditions

Free – free (F – F) boundary conditions are given by [4]

$$N_x = 0 \qquad N_{x\theta} + \frac{M_{x\theta}}{R} = 0 \qquad M_x = 0 \qquad Q_x + \frac{1}{R}\frac{\partial M_{x\theta}}{\partial \theta} = 0 \qquad \text{for} \quad \eta = 0,1 \qquad (27)$$

where forces and moments are given by [4]

$$N_x = \frac{Eh}{1-\nu^2}\left(\varepsilon_{x,0} + \nu\varepsilon_{\theta,0}\right) \quad N_{x\theta} = \frac{Eh}{2(1+\nu)}\gamma_{x\theta,0} \quad M_x = \frac{Eh^3}{12(1-\nu^2)}\left(k_x + \nu k_\theta\right)$$

$$M_{x\theta} = \frac{Eh^3}{24(1+\nu)}k_{x\theta} \qquad Q_x = \frac{Eh^3}{12(1-\nu^2)}\left(k_{x,x} + \nu k_{\theta,x}\right) + \frac{Eh^3}{24(1+\nu)}k_{x\theta,\theta} \qquad (28)$$

In this case, all the boundary conditions are "natural", i.e., they involve essentially "forces". In such a case, it is well known that the Ritz procedure can be applied even if the natural boundary conditions are not respected; therefore, here no boundary conditions are imposed for the free-free case.

Linear Vibration Analysis: Rayleigh-Ritz Procedure

The maximum number of variables needed for describing a generic vibration mode can be calculated by the following relation $\left(N_p = M_u + M_v + M_w + 3 - r\right)$, with $(M_u = M_v = M_w)$ as maximum degree of the Chebyshev polynomials and r as number of equations for the boundary conditions considered.

For a multi-mode analysis including different nodal diameters, the number of degrees of freedom of the system is computed by the relation $\left(N_{max} = N_p \times (N+1)\right)$, where N describes the maximum number of nodal diameters considered.

Equations (15) are inserted in the expressions of U_s and T_s (Eqns. $(11-12)$).

Consider now the Rayleigh quotient $R(\tilde{\mathbf{q}}) = \frac{V_{max}}{T^*}$, where V_{max} is the maximum of the potential energy, $T^* = \frac{T_{max}}{\omega^2}$, T_{max} is the maximum of the kinetic energy, ω is the circular frequency of the harmonic motion, $\tilde{\mathbf{q}} = \left[\ldots, \tilde{U}_{m,n}, \tilde{V}_{m,n}, \tilde{W}_{m,n}, \ldots\right]^T$ is a vector containing all the unknowns.

After imposing the stationarity to the Rayleigh quotient, one obtains the eigenvalue problem [8]

$$(-\omega^2\mathbf{M} + \mathbf{K})\tilde{\mathbf{q}} = \mathbf{0} \qquad (29)$$

which furnishes natural frequencies and modes of vibration (eigenvalues and eigenvectors) of the system.

The modal shape is given by the Eqns. (16), where coefficients $(\tilde{U}_{m,n}, \tilde{V}_{m,n}, \tilde{W}_{m,n})$ are substituted with $(\tilde{U}^{(j)}_{m,n}, \tilde{V}^{(j)}_{m,n}, \tilde{W}^{(j)}_{m,n})$, which are the components of the j-th eigenvector $\tilde{\mathbf{q}}_\mathrm{j}$ of the Eqn. (29).

The vector function $\boldsymbol{U}^{(j)}(\eta,\theta) = \left[U^{(j)}(\eta,\theta), V^{(j)}(\eta,\theta), W^{(j)}(\eta,\theta)\right]^T$ represents an approximation of the j-th mode of the original problem; the eigenfunctions obtained are normalized by imposing $max\left[max\left[U^{(j)}(\eta,\theta)\right], max\left[V^{(j)}(\eta,\theta)\right], max\left[W^{(j)}(\eta,\theta)\right]\right] = 1$, see Ref. [8] for explanation.

Nonlinear Vibration Analysis: Lagrange Equations

In the nonlinear vibration analysis, the full expression of the elastic strain energy (11), containing terms up to the fourth order (cubic nonlinearity), is considered.

The displacement fields $u(\eta,\theta,t), v(\eta,\theta,t), w(\eta,\theta,t)$ are then expanded by using the linear mode shapes $U(\eta,\theta), V(\eta,\theta), W(\eta,\theta)$ obtained in the previous section [8]

$$u(\eta,\theta,t) = \sum_{j=1}^{N_u} U^{(j)}(\eta,\theta) f_{u,j}(t)$$

$$v(\eta,\theta,t) = \sum_{j=1}^{N_v} V^{(j)}(\eta,\theta) f_{v,j}(t)$$

$$w(\eta,\theta,t) = \sum_{j=1}^{N_w} W^{(j)}(\eta,\theta) f_{w,j}(t) \tag{30}$$

These expansions respect exactly the boundary conditions except for the free case; the synchronicity is relaxed as for each mode and each component (u, v, w) different time laws are allowed.

Mode shapes $U^{(j)}(\eta,\theta), V^{(j)}(\eta,\theta), W^{(j)}(\eta,\theta)$ are known functions expressed in terms of polynomials and harmonic functions.

The Lagrange equations for forced vibrations are expressed in the following form [8]

$$\frac{d}{dt}\left(\frac{\partial L}{\partial \dot{q}_i}\right) - \frac{\partial L}{\partial q_i} = Q_i \qquad \text{for } i\epsilon[1, N_{max}] \qquad (L = T_s - U_s) \tag{31}$$

where the modal coordinates are now ordered in a vector $\mathbf{q}(t) = [\dots f_{u,j}, f_{v,j}, f_{w,j}, \dots]$, N_{max} depends on the number of modes considered in the expansions (30).

The generalized forces Q_i are obtained by differentiation of the Rayleigh's dissipation function F (14) and the virtual work done by external forces W (13), in the form [8]

$$Q_i = -\frac{\partial F}{\partial \dot{q}_i} + \frac{\partial W}{\partial q_i} \tag{32}$$

Expansions (30) are inserted into strain energy (11), kinetic energy (12), virtual work of the external forces (13) and damping forces (14).

Using Lagrange Eqns. (31), a set of nonlinear ordinary differential equations (ODE) is then obtained.

5. NUMERICAL RESULTS

In this section, the nonlinear vibrations of functionally graded circular cylindrical shells with different modal shape expansions, geometries and boundary conditions are analyzed.

Analyses are carried out on an FGM made of stainless steel and nickel.

FGM properties are graded in the thickness direction according to a volume fraction distribution, where p is the power-law exponent.

The material properties against coefficients of temperature at $T = 300\text{K}$ are reported in Tab. 1 [2].

Table 1. Properties of stainless steel and nickel against coefficients of temperature.

	stainless steel			nickel		
	E	ν	ρ	E	ν	ρ
P_0	2.0×10^{11} Nm^{-2}	0.326	8166 kgm^{-3}	2.2×10^{11} Nm^{-2}	0.310	8900 kgm^{-3}
P_{-1}	0 K	0 K	0 K	0 K	0 K	0 K
P_1	3.1×10^{-4} K^{-1}	-2.0×10^{-4} K^{-1}	0 K^{-1}	-2.8×10^{-4} K^{-1}	0 K^{-1}	0 K^{-1}
P_2	-6.5×10^{-7} K^{-2}	3.8×10^{-7} K^{-2}	0 K^{-2}	-4.0×10^{-9} K^{-2}	0 K^{-2}	0 K^{-2}
P_3	0 K^{-3}	0 K^{-3}	0 K^{-3}	0 K^{-3}	0 K^{-3}	0 K^{-3}
P	2.1×10^{11} Nm^{-2}	0.318	8166 kgm^{-3}	2.0×10^{11} Nm^{-2}	0.310	8900 kgm^{-3}

Nonlinear Response Convergence Analysis

The convergence analysis is carried out on a simply supported cylindrical shell excited with an harmonic force; the excitation frequency is close to the mode (m, n).

The convergence is checked by adding suitable modes to the resonant one:
asymmetric modes $(k \times m, j \times n)$ $k = 1,3$ $j = 1,2,3$ due to the presence both of quadratic and cubic nonlinearities;
axisymmetric modes $(k, 0)$ $k = 1,3,5,7$ due to the quadratic nonlinearities.

The convergence analysis is then developed by introducing a different number of asymmetric and axisymmetric modes in the expansions of the displacement fields u, v, w, see Tab. 2.

The FGM cylindrical shell is excited by means of an external modally distributed radial force $q_z = f_{1,6} \sin\eta \cos 6\theta \cos\Omega t$; the amplitude of excitation is $f_{1,6} = 0.0012h^2\varrho\omega_{1,6}^2$ and the frequency of excitation Ω is close to the mode $(1,6)$, $\Omega \cong \omega_{1,6}$.

The external forcing $f_{1,6}$ is normalized with respect to mass, acceleration and thickness; the damping ratio is equal to $\xi_{1,6} = 0.0005$.

The nonlinear amplitudes $f_{u,1}, f_{v,1}, f_{w,1}$ of expansions (30) refer to the displacement fields u, v, w of the mode $(1,6)$, respectively.

In Figure 2, a comparison of nonlinear amplitude-frequency curves of the cylindrical shell $(h/R = 0.002, L/R = 20, p = 1)$ with different nonlinear expansions is shown; the shell is very thin and long.

The nonlinear 6 dof model describes a wrong softening nonlinear behaviour, while the higher-order nonlinear expansions converge to a hardening nonlinear behaviour.

Higher- order models (dof from 9 to 18) behave quite similarly, this means that in this case the accuracy is acceptable for the 9 dof model.

Table 2. Asymmetric and axisymmetric modes inserted in the different nonlinear models.

6 dof model	9 dof model	12 dof model	15 dof model	18 dof model
mode (1,6) u, v, w	mode (1,6) u, v, w	mode (1,6) u, v, w	mode (1,6) u, v, w	mode (1,6) u, v, w
mode (1,12) v	mode (1,12) v	mode (3,6) u, v, w	mode (3,6) u, v, w	mode (3,6) u, v, w
mode (1,0) u, w	mode (3,12) v	mode (1,12) v	mode (1,12) v	mode (1,12) v
	mode (1,0) u, w	mode (3,12) v	mode (3,12) v	mode (3,12) v
	mode (3,0) u, w	mode (1,0) u, w	mode (1,18) v	mode (1,18) v
		mode (3,0) u, w	mode (1,0) u, w	mode (3,18) v
			mode (3,0) u, w	mode (1,0) u, w
			mode (5,0) u, w	mode (3,0) u, w
				mode (5,0) u, w
				mode (7,0) u, w

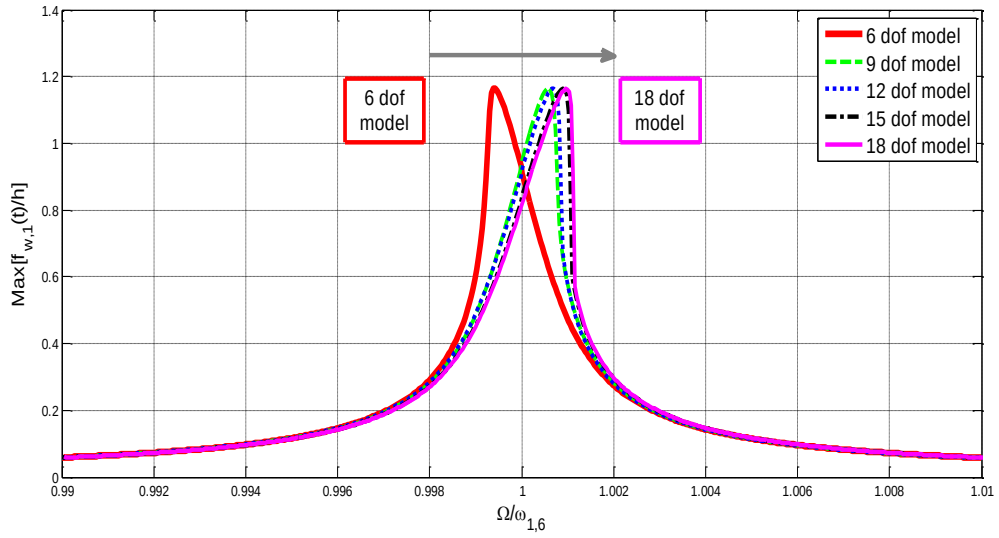

Figure 2. Comparison of nonlinear amplitude-frequency curves of the cylindrical shell ($h/R = 0.002, L/R = 20, p = 1$). "■", 6 dof model; "– –", 9 dof model; "…", 12 dof model; "– · –", 15 dof model; "–", 18 dof model.

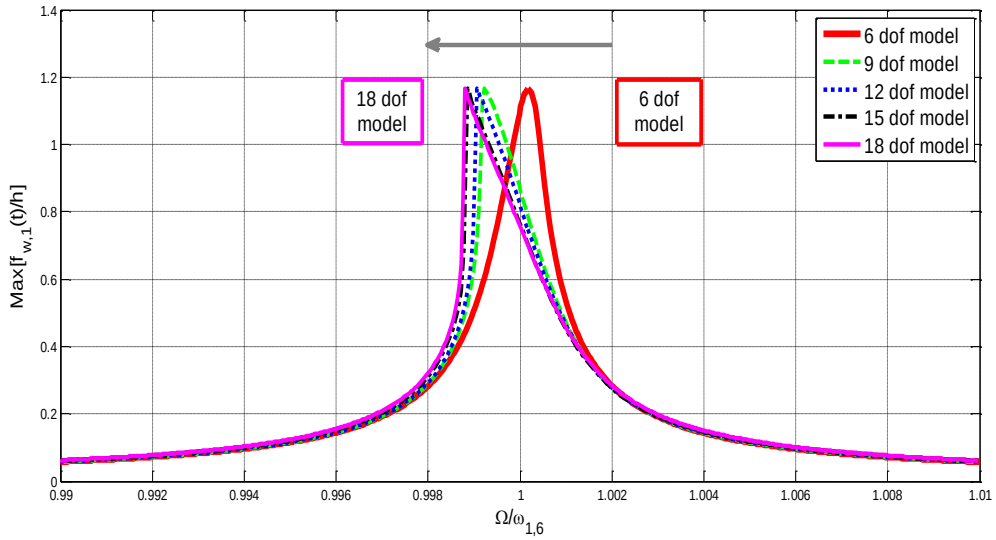

Figure 3. Comparison of nonlinear amplitude-frequency curves of the cylindrical shell ($h/R = 0.025, L/R = 20, p = 1$). "■", 6 dof model; "– –", 9 dof model; "…", 12 dof model; "– · –", 15 dof model; "–", 18 dof model.

In Figure 3, a comparison of nonlinear amplitude-frequency curves of the cylindrical shell $(h/R = 0.025, L/R = 20, p = 1)$ with different nonlinear expansions is shown; the shell is moderately thick and long.

The nonlinear 6 dof model describes a wrong slightly hardening nonlinear behaviour, the higher-order nonlinear expansions converge to a softening nonlinear behaviour.

Also in this case, the models having 9-18 dof behave quite similarly.

In Figure 4, a comparison of nonlinear amplitude-frequency curves of the cylindrical shell $(h/R = 0.050, L/R = 20, p = 1)$ with different nonlinear expansions is shown: the nonlinear 6 dof model describes a wrong softening nonlinear behaviour, the higher-order nonlinear expansions converge to a hardening nonlinear behaviour.

The shell is slightly thicker than that of Fig. 3, but now the behaviour is hardening.

From these convergence analyses, one can say that the 9 dof model gives satisfactory results with the minimal computational effort; therefore, in the following, the 9 dof model will be used.

Considering a generic resonant mode (m, n), the expansion is:

- modes $(m, n), (1,0), (3,0)$ in the longitudinal displacement field u
- modes $(m, n), (m, 2n), \ (3m, 2n)$ in the circumferential displacement field v
- modes $(m, n), (1,0), (3,0)$ in the radial displacement field w

After selecting such modes, each expansion present in the Eqns. (30) is reduced to a three-terms modal expansion; the resulting nonlinear system has 9 dof.

It is to note that the present convergence analysis confirms the results available in the literature: in the nonlinear field, axisymmetric modes play a role of primary importance.

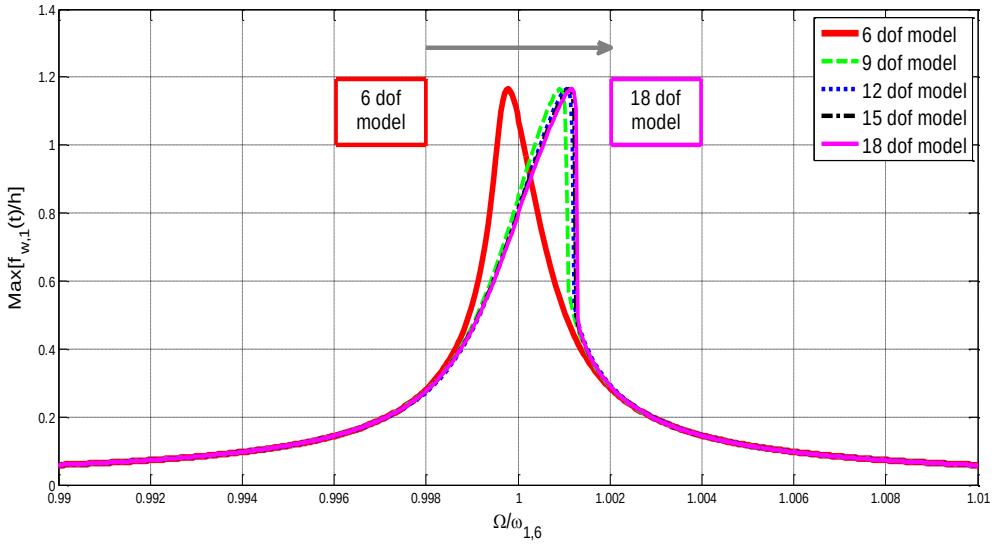

Figure 4. Comparison of nonlinear amplitude-frequency curves of the cylindrical shell $(\mathrm{h/R} = 0.050, \mathrm{L/R} = 20, \mathrm{p} = 1)$. "■", 6 dof model; "– –", 9 dof model; "…", 12 dof model; "– · –", 15 dof model; "–", 18 dof model.

Effect of the Boundary Conditions on the Nonlinear Response

In the present section, the effect of the boundary conditions on the natural frequencies and nonlinear responses of the shells is analyzed. Simply supported – simply supported (S – S), clamped – clamped (C – C), clamped – simply supported (C – S), clamped – free (C – F), simply supported – free (S – F) and free – free (F – F) boundary conditions are considered.

In Figure 5, the natural frequencies of the FGM shell $(h/R = 0.002, L/R = 20, p = 1)$ under various boundary conditions are shown.

For all the six boundary conditions, the frequencies initially decrease and then increase as the circumferential wavenumber n increases (number of longitudinal half-waves $m = 1$).

For all the boundary conditions, the minimum frequency occurs in between $n = 2$ and $n = 4$ (note that the minimum is also influenced by the ratios h/R and L/R); the natural frequencies converge for $n > 6$, i.e., the effect of the boundary conditions on the natural frequencies is prominent for low circumferential wavenumbers $n \in [1,5]$ and disappears for higher circumferential wavenumbers, when the corresponding six natural frequency curves merge into a single curve.

In particular, for $n \in [1,5]$, the value of the natural frequency for the F – F shell is the highest one, followed by the C – F, C – C, S – F, C – S and S – S values, in that order.

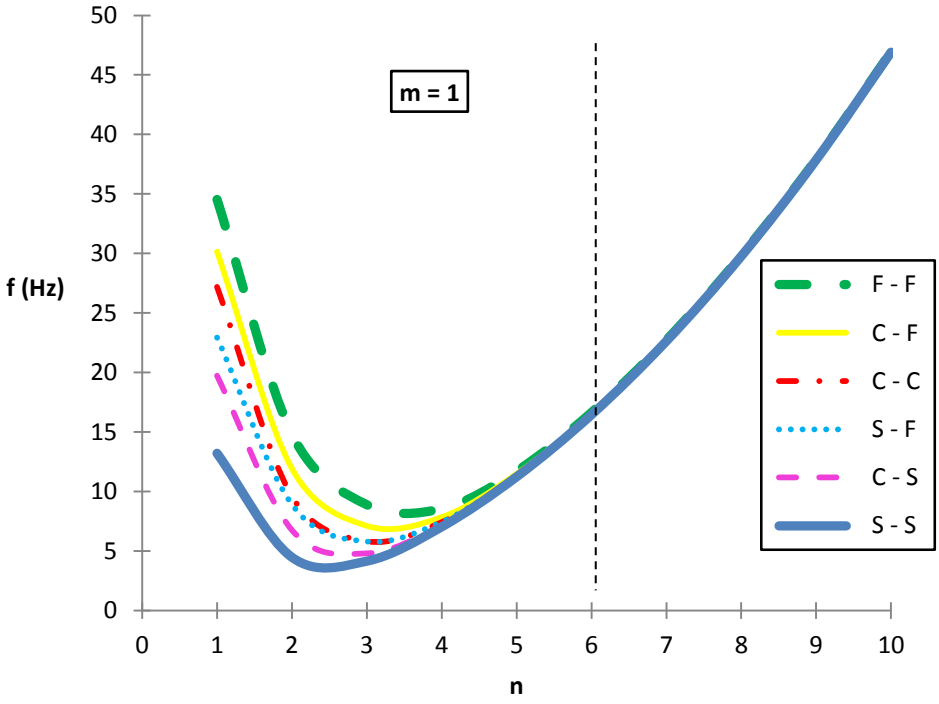

Figure 5. Variation of natural frequencies of the shell $(h/R = 0.002, L/R = 20, p = 1)$. "■■", Free – Free; "—", Clamped – Free; "– · –", Clamped – Clamped; "···", Simply – Free; "– –", Clamped – Simply; "■", Simply – Simply.

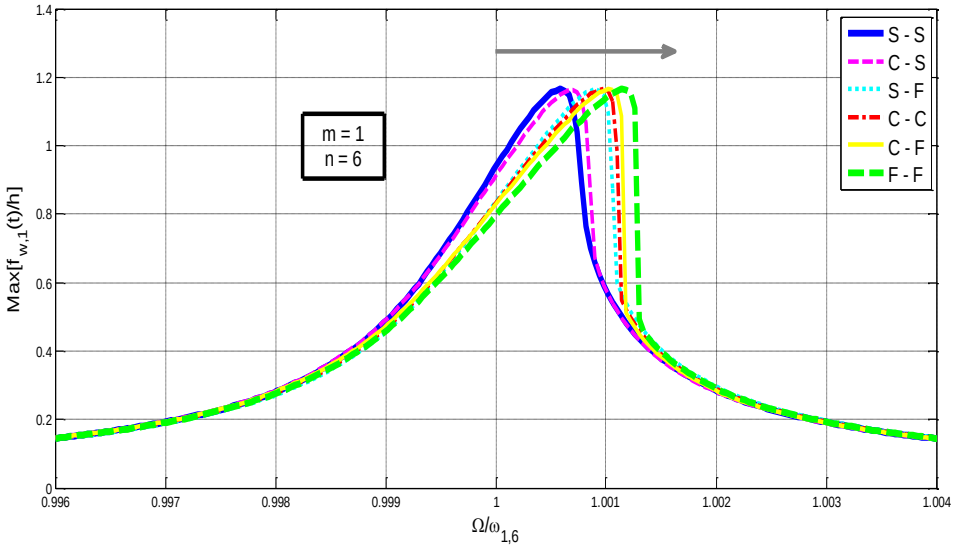

Figure 6. Comparison of nonlinear amplitude-frequency curves of the cylindrical shell $(\mathrm{h/R} = 0.002, \mathrm{L/R} = 20, \mathrm{p} = 1)$. "■", Simply – Simply; "– · –", Clamped – Clamped; "■■", Free – Free; "– –", Clamped – Simply; "—", Clamped – Free; "···", Simply – Free.

In Figure 6, a comparison of nonlinear amplitude-frequency curves of the cylindrical shell $(h/R = 0.002, L/R = 20, p = 1)$ for the driven mode $(1,6)$ is shown; six different boundary conditions are analyzed: the S – S and C – S behave similarly, the S – F, C – C and C – F behave similarly, the F – F gives the strongest nonlinearity.

6. CONCLUSIONS

In this paper, the nonlinear vibrations of FGM circular cylindrical shells are analyzed; the Sanders-Koiter theory is applied to model the nonlinear dynamics of the system in the case of finite amplitude of vibration.

The functionally graded material is made of a uniform distribution of stainless steel and nickel, and the material properties are graded in the thickness direction, according to a volume fraction power-law distribution.

Numerical analyses are carried out in order to characterize the nonlinear response when the shell is subjected to a harmonic external load.

A convergence analysis is carried out by introducing in longitudinal, circumferential and radial displacement fields a different number of asymmetric and axisymmetric modes; the fundamental role of the axisymmetric modes is confirmed, and the role of the higher-order asymmetric modes is clarified in order to obtain the actual character of nonlinearity.

The effect of the boundary conditions on the natural frequencies and nonlinear responses of the shells is analyzed. The effect of the boundary conditions on the natural frequencies is prominent for the low circumferential wave numbers, and disappears for high circumferential wave numbers. The boundary conditions strongly influence the nonlinear character of the shell response.

REFERENCES

[1] Technical Report, Japanese Government, 1987. Research on the Basic Technology for the Development of Functionally Gradient Materials for Relaxation of Thermal-stress. Science and Technology Agency of Japanese Government.

[2] Loy CT, Lam KY, and Reddy JN, 1999. "Vibration of functionally graded cylindrical shells". *International Journal of Mechanical Sciences,* **41**, pp. 309–324.

[3] Pradhan SC, Loy CT, Lam KY, and Reddy JN, 2000. "Vibration characteristics of functionally graded cylindrical shells under various boundary conditions". *Applied Acoustics,* **61**, pp. 111–129.

[4] Leissa AW, 1973. *Vibrations of Shells*. Government Printing Office, Washington DC.

[5] Yamaki N, 1984. *Elastic Stability of Circular Cylindrical Shells*. North-Holland, Amsterdam.

[6] Amabili M, 2008. *Nonlinear Vibrations and Stability of Shells and Plates*. Cambridge University Press, New York.

[7] Pellicano F, Amabili M, and Paidoussis MP, 2002. "Effect of the geometry on the non-linear vibration of circular cylindrical shells". *International Journal of Nonlinear Mechanics,* **37**, pp. 1181–1198.

[8] Pellicano F, 2007. "Vibrations of circular cylindrical shells: Theory and experiments". *Journal of Sound and Vibration,* **303**, pp. 154–170.

[9] Kurylov Y, Amabili M, 2010. "Polynomial versus trigonometric expansions for nonlinear vibrations of circular cylindrical shells with different boundary conditions". *Journal of Sound and Vibration,* **329**, pp. 1435–1449.

[10] Zhang L, Xiang Y, and Wei GW, 2006. "Local adaptive differential quadrature for free vibration analysis of cylindrical shells with various boundary conditions". *International Journal of Mechanical Sciences,* **48**, pp. 1126–1138.